Theor Chem Account (2007) 118:709–721
DOI 10.1007/s00214-007-0350-2

REGULAR ARTICLE

Chemical forces in terms of the electron density

J. Fernández Rico · R. López · I. Ema · G. Ramírez

Received: 22 December 2006 / Accepted: 9 March 2007 / Published online: 11 July 2007
© Springer-Verlag 2007

Abstract A previous study of the small deformations produced by the molecular environment in the atomic densities has concluded that these deformations reflect and support all the concepts of the empirical structural chemistry. In the present work the study is extended to the chemical forces. Four types are distinguished: Van der Waals, Pauli, bonding and nuclear unscreening forces. For each type, the origin, the associated density deformations, the force generated by these deformations and the main role played by this force are investigated. It is stressed that Van der Waals complexes, usual molecules, conformers and chemical processes can be described in terms of these four forces, and are determined by the balance between them. It is proved that simple models for the density are often sufficient for semiquantitative predictions of forces, and can be very helpful for rationalizing the chemical properties and behavior. Developments are illustrated and supported with specific examples.

Keywords Serafín Fraga · Hellmann–Feynman · Molecular forces · Molecular density · Electrostatic theorem

1 Introduction

In 1928, P.A.M. Dirac wrote a celebrated sentence: *The underlying physical laws necessary for the mathematical theory of a large part of physics and the whole of chemistry are thus completely known, and the difficulty is only that the exact application of these laws leads to equations much too complicated to be soluble*. Around the 1960s, when computers started to be accesible to the scientific community, a group of young researchers faced the task of establishing firmly grounded theoretical methods, algorithms and computational programs for the application of those laws to chemistry. Prof. S. Fraga played an outstanding role in this exciting intelectual adventure. As recently reported [1] by a leader of this movement, E. Clementi, they succeded: a new branch of chemistry (Computational Chemistry) was born, and a new powerful tool was made available to chemists for investigating the properties of matter.

Nevertheless, Computational Chemistry does not exhaust the possibilities of Quantum Mechanics in chemistry. It is worldwide known that concepts, laws and language of chemistry were mostly developed on an empirical basis before the advent of Quantum Mechanics and, since the latter has the capabilities for explaining the whole chemistry, it should be able to give a theoretical support for them.

This fact was recognized in the early years of Quantum Mechanics (1930s–1950s) when Heitler, London, Pauling, Hellmann, Feynman, and many more made important contributions in this direction. However, in the following decades (from the 1960s on) the effort was moved towards computational aspects, and the findings of the previous period were gradually relegated, with few valuable exceptions, to the status of scientific curiosities.

Among these exceptions, we consider specially relevant the papers on the interpretation of the chemical behavior in terms of electron density and forces by Coulson [2], Hurley [3–5], Berlin [6], Politzer [7,8], Bader [9–11], Stone [12], and Deb [13]. This research line, very active in the late 1960s and early 1970s was almost abandoned in the following years,

---

Contribution to the Serafin Fraga Memorial Issue.

Financial support: Dirección General de Investigación Científica y Técnica (CTQ2004-06615/BQU).

J. Fernández Rico (✉) · R. López · I. Ema · G. Ramírez
Departamento de Química Física Aplicada,
Facultad de Ciencias C-XIV, Universidad Autónoma de Madrid,
28049 Madrid, Spain
e-mail: jaime.fernandez@uam.es

probably due to the lack of suitable tools for exploring its full capabilities. Our work takes on this line profitting from recent progress in these tools [14–21].

Analyzing the implications of the Hellmann–Feynman theorem [22,23], we have recently stressed [24] the basic role played in the chemical behavior by the small deformations caused in the atomic densities by the molecular environment. Moreover, we have studied [25] these deformations in an ample set of molecules and proved that they reflect and support all basic concepts of the empirical structural chemistry. The relationship between lone pairs, single, double and triple bonds, functional groups and so forth, with the density deformations being so tight that one can regard these chemical concepts as a symbolic representation of the latter.

In this paper, we extend the analysis to the chemical forces, i.e., to the forces acting on the nuclei. In the Born–Oppenheimer approximation (the paradigm of theoretical chemistry), these forces can be rigorously defined in two equivalent ways: from the derivatives of the electronic energy (including the nuclear repulsion) or from the electrostatic force exerted on nuclei by the whole charge distribution (electron density plus nuclear charges) of the molecule.

The first way only gives the net force on nuclei, being scarcely useful for descriptive and interpretative purposes. On the contrary, the second is plenty of chemical insight because it enables to know how forces depend on the shape of the charge distribution, and how parts of a system affect the forces acting on other parts.

It can be argued that, since physical effects are determined by net forces, every decomposition of them is arbitrary and useless. Note, however, that the decomposition of a force is not only correct but it is the usual way (and often the only way) to understand the forces acting in complex systems.

In this work we will stress that, in a nonrelativistic approach, chemical behavior can be described in terms of four basic forces: Van der Waals, Pauli, bonding and nuclear unscreening. We will also note that these four types of forces arise from the electron density, and examine and illustrate with specific examples which are the components of the density associated to everyone.

2 Chemical forces: general approach

Let $\widehat{\mathcal{H}}$ be the electronic Hamiltonian of a molecule with n electrons, N nuclei and an external potential

$$V = \sum_{i=1}^{n} v(\mathbf{r}_i) \tag{1}$$

$$v(\mathbf{r}) = -\sum_{A=1}^{N} \frac{\zeta_A}{|\mathbf{r} - \mathbf{R}_A|} \tag{2}$$

where ζ_A denotes the nuclear charge and $\mathbf{R}_A = X_A\,\mathbf{i} + Y_A\,\mathbf{j} + Z_A\,\mathbf{k}$ the nuclear position.

Following the Born–Oppenheimer prescription, one must solve

$$\widehat{\mathcal{H}}\,\Psi = E\,\Psi \tag{3}$$

and use

$$E_T = E + V_N = E + \sum_{A=1}^{N} \sum_{B<A} \frac{\zeta_A\,\zeta_B}{|\mathbf{R}_B - \mathbf{R}_A|} \tag{4}$$

as the potential energy for nuclear motion. With this potential, the usual definition of force gives

$$\mathbf{F}_A = -\boldsymbol{\nabla}_A E_T \tag{5}$$

where

$$\boldsymbol{\nabla}_A = \mathbf{i}\,\frac{\partial}{\partial X_A} + \mathbf{j}\,\frac{\partial}{\partial Y_A} + \mathbf{k}\,\frac{\partial}{\partial Z_A}. \tag{6}$$

Since E changes with every parameter of $v(\mathbf{r})$, one can write $E \equiv E(\mathbf{R}_1, \zeta_1, \ldots, \mathbf{R}_N, \zeta_N)$ and similar expressions for E_T and $\mathbf{F}_A$, but the invariance of E under translation and rotation of the axes system introduces six constraints that reduce the number of independent parameters to $3N - 6$ related to nuclear positions and N to nuclear charges. These constraints, can be expressed in terms of forces

$$\sum_{A=1}^{N} \boldsymbol{\nabla}_A E_T = 0 \quad \Longleftrightarrow \quad \sum_{A=1}^{N} \mathbf{F}_A = 0 \tag{7}$$

$$\sum_{A=1}^{N} \mathbf{R}_A \times \boldsymbol{\nabla}_A E_T = 0 \quad \Longleftrightarrow \quad \sum_{A=1}^{N} \mathbf{R}_A \times \mathbf{F}_A = 0 \tag{8}$$

thus ensuring that the total force and torque of the system are zero.

The forces of Eq. 5 are related to the electron density through the Hellmann–Feynman theorem [22,23] which, according to Slater [26], is one of the most powerful theorems applicable to molecules. It can be derived in several equivalent ways [13,27], but all of them lead to

$$\frac{\partial E(\boldsymbol{\lambda})}{\partial \lambda_p} = \int d\mathbf{r}\; \rho(\mathbf{r}, \boldsymbol{\lambda})\, \frac{\partial v(\mathbf{r}, \boldsymbol{\lambda})}{\partial \lambda_p} \tag{9}$$

which is the Hellmann–Feynman theorem for λ_p, $\rho(\mathbf{r}, \boldsymbol{\lambda})$ being the electron density, $\boldsymbol{\lambda}$ being the set of parameters on which it depends.

Taking the space coordinates of nucleus A as parameters, the theorem gives

$$\mathbf{F}_A = -\boldsymbol{\nabla}_A E_T = -\int d\mathbf{r}\; \rho(\mathbf{r}, \boldsymbol{\lambda})\; \boldsymbol{\nabla}_A v(\mathbf{r}, \boldsymbol{\lambda}) - \boldsymbol{\nabla}_A V_N \tag{10}$$

In a fixed conformation, Eq. 10 reads

$$\mathbf{F}_A = \zeta_A \int \mathrm{d}\mathbf{r}\ \rho(\mathbf{r},\boldsymbol{\lambda}) \frac{\mathbf{r}-\mathbf{R}_A}{|\mathbf{r}-\mathbf{R}_A|^3} - \zeta_A \sum_{B \neq A} \zeta_B \frac{\mathbf{R}_B-\mathbf{R}_A}{|\mathbf{R}_B-\mathbf{R}_A|^3} \tag{11}$$

so that the force on nucleus A is the classical electrostatic force exerted on A by the electron cloud and the remaining nuclei.

We will consider now a configurational or reactive process in which the nuclei move along the path determined by a parameter μ: $\mathbf{R}_I(\mu) = \mathbf{i}\,X_I(\mu) + \mathbf{j}\,Y_I(\mu) + \mathbf{k}\,Z_I(\mu)$ and let μ_1 and μ_2 be two values of the path parameter. Then, the energy difference between the corresponding conformations is

$$\begin{aligned}\Delta E_T &= \int_{\mu_1}^{\mu_2} \mathrm{d}\mu \int \mathrm{d}\mathbf{r}\ \rho(\mathbf{r},\mu)\ \frac{\partial}{\partial\mu} v(\mathbf{r},\mu) + \Delta V_N \\ &= \int_{\mu_1}^{\mu_2} \mathrm{d}\mu \sum_{A=1}^{N} \mathbf{F}_A(\mu)\ \frac{\partial \mathbf{R}_A(\mu)}{\partial\mu}\end{aligned} \tag{12}$$

where the last equality comes from

$$\frac{\partial}{\partial\mu} v(\mathbf{r},\mu) = \sum_{A=1}^{N} (\nabla_A v)\ \frac{\partial \mathbf{R}_A}{\partial\mu}. \tag{13}$$

This is the integrated Hellmann–Feynman (electrostatic) theorem, again a classical expression that relates variations of energy with the work done by electrostatic forces.

The first integral of Eq. 12 can be eliminated with the following argument. Let $E(\mu_1)$, $\Psi(\mu_1)$ and $E(\mu_2)$, $\Psi(\mu_2)$ be the initial and final energies and wavefunctions. Multiplying the eigenvalue equation at μ_1 by $\Psi(\mu_2)$, and that at μ_2 by $\Psi(\mu_1)$, integrating with respect to the electron coordinates, and subtracting the resulting expressions, one finds

$$\Delta E = S_{21}^{-1} \int \mathrm{d}\mathbf{r}\ \rho_{21}(\mathbf{r})\ v_{21}(\mathbf{r}) \tag{14}$$

where S_{21} is the overlap of $\Psi(\mu_1)$ and $\Psi(\mu_2)$, $\rho_{21}(\mathbf{r})$ is the transition density involving these functions, and $v_{21}(\mathbf{r}) = v(\mathbf{r},\mu_2) - v(\mathbf{r},\mu_1)$.

This is the integral Hellmann–Feynman theorem [28,29], which relates the difference of the electronic energy at two conformations with the change in the *electrostatic* energies of the nuclei, at fixed electron cloud determined by the normalized transition density.

Apart from the theoretical implications [30], the Hellmann–Feynman theorem is a cornerstone in the interpretation of the chemical bond. Note for instance that there is an extended tendency to explain the bond directly from the features of the kinetic energy or the electron repulsion. However, by deriving the usual expression of the energy and using Eq. 9 one finds

$$\begin{aligned}0 = \int \mathrm{d}\mathbf{r}\ v(\mathbf{r},\boldsymbol{\lambda})\ \frac{\partial\rho(\mathbf{r},\boldsymbol{\lambda})}{\partial\lambda_p} + \int \mathrm{d}\mathbf{r} \int \mathrm{d}\mathbf{r}' \Bigg[\delta(\mathbf{r}-\mathbf{r}') \\ \times \frac{1}{2}\ \nabla\,\nabla'\ \frac{\partial\widehat{\rho}(\mathbf{r},\mathbf{r}',\boldsymbol{\lambda})}{\partial\lambda_p} + \frac{\partial}{\partial\lambda_p}\ \frac{\Gamma(\mathbf{r},\mathbf{r}',\boldsymbol{\lambda})}{|\mathbf{r}-\mathbf{r}'|}\Bigg]\end{aligned} \tag{15}$$

where $\widehat{\rho}(\mathbf{r},\mathbf{r}',\boldsymbol{\lambda})$ is the density matrix and $\Gamma(\mathbf{r},\mathbf{r}',\boldsymbol{\lambda})$ is the pairs density. From Eq. 15, it follows that kinetic energy and electron repulsion are part of a constant along any conformational or reactive change (i.e., during the bond formation or breaking), and hence their changes cannot be directly responsible [31] for any change in the electron energy. The effect of these properties on energy is indirect: to know it, one must determine how they influence the density and analyze whether this influence gives rise to attractive forces or not.

As remarked before, the forces can be calculated from the energy [32] Eq. 9 or from the density Eq. 14. For the exact energy and density both ways give the same results, but this does not necessarily hold for approximated energy and density. In this case, one is faced with two different problems: how near are both sets of approximate forces, $\mathbf{F}_A(\rho^{(ap)})$ and $\mathbf{F}_A(E^{(ap)})$, to the exact ones $\mathbf{F}_A$, and how near are to one another.

Since in a variational calculation, error boundary is unknown, it is not possible to answer the first question unless the exact forces are known, but the second question is affordable. In this regard, it is usually said that *the Hellmann–Feynman theorem is strictly fulfilled when the forces obtained from the gradient of an approximate energy equal those computed from the corresponding approximate density*.

The fulfillment of the electrostatic theorem was first studied by Hurley [3–5] and next by other authors [33–38] in terms of conditions on the basis sets that are not satisfied by the ones usually employed. Notice, however, that the important question in practice is the degree of fulfillment, which determines whether the electrostatic forces are sufficiently accurate to replace the energy gradient.

Following a pioneer work by Nakatsuji [39] on this subject, the problem has been recently readdressed [20,21] to the search of criterions for obtaining moderate size basis sets of the usual type with a high degree of fulfillment of the theorem, and today high performance basis sets of Slater [21] and Gaussian [40] types are available.

To end this section, we want to stress that Eqs. (11) and (12) evince the deep understanding of a chemical process provided by its approach from density. One can know not only the variations of energy but also the driving forces of the process, their contributions to the energy variation, what components of the density are responsible for these forces and how they are, where they are localized, and so forth. Clearly, suitable partitions of the density can be very helpful in this analysis but, when choosing them, one must be aware that *the essential point in the density/forces/energy relationships is how the density evolves when the* $\boldsymbol{\lambda}$ *parameters vary*—i.e., how $\rho(\mathbf{r},\boldsymbol{\lambda})$ depends on $\boldsymbol{\lambda}$—whereas most current descriptions are aimed at analyzing the dependence of $\rho(\mathbf{r},\boldsymbol{\lambda})$ with $\mathbf{r}$ at fixed $\boldsymbol{\lambda}$.

3 Van der Waals forces in terms of density

Let Ψ^{α}, E_T^{α} and Ψ^{β}, E_T^{β} be the electronic wavefunctions and energies of two isolated systems containing, respectively, n_α and n_β electrons and N_α and N_β nuclei.

Assuming constant nuclear charges Ψ^{α}, E_T^{α} and Ψ^{β}, E_T^{β} will depend, respectively, on $3N_\alpha-6$ and $3N_\beta-6$ parameters, $\boldsymbol{\lambda}^{\alpha}=(\lambda_1^{\alpha},\ldots,\lambda_{3N_\alpha-6}^{\alpha})$ and $\boldsymbol{\lambda}^{\beta}=(\lambda_1^{\beta},\ldots,\lambda_{3N_\beta-6}^{\beta})$, and each of their sets of $3N_\alpha$ and $3N_\beta$ forces will be constrained by six equalities like (7) and (8).

Let us consider now their adduct. Assigning electrons 1 to n_α to $\widehat{\mathcal{H}}^{\alpha}$ and $n_\alpha+1$ to $n_\alpha+n_\beta$ to $\widehat{\mathcal{H}}^{\beta}$, the electron hamiltonian can be written

$$\widehat{\mathcal{H}}^{\alpha\beta}=\widehat{\mathcal{H}}^{\alpha}+\widehat{\mathcal{H}}^{\beta}+\widehat{\mathcal{H}}^{\alpha\beta}_{\text{int}} \tag{16}$$

with

$$\widehat{\mathcal{H}}^{\alpha\beta}_{\text{int}}=-\sum_{i=1}^{n_\alpha}\sum_{B=1}^{N_\beta}\frac{\zeta_B}{|\mathbf{r}_i-\mathbf{R}_B|}-\sum_{j=n_\alpha+1}^{n_\alpha+n_\beta}\sum_{A=1}^{N_\alpha}\frac{\zeta_A}{|\mathbf{r}_j-\mathbf{R}_A|}+\sum_{i=1}^{n_\alpha}\sum_{j=n_\alpha+1}^{n_\alpha+n_\beta}\frac{1}{|\mathbf{r}_i-\mathbf{r}_j|} \tag{17}$$

Since the adduct has N_A+N_B nuclei, the eigenfuctions, $\Psi^{\alpha\beta}$, and eigenvalues, $E^{\alpha\beta}$, of $\widehat{\mathcal{H}}^{\alpha\beta}$ depend on $3N_\alpha+3N_\beta-6$ parameters. With respect to the isolated systems, there are six additional degrees of freedom that, attaching somehow parallel axis systems to the two subsets of nuclei, can be associated to the relative translation and rotation of these systems.

Let us suppose that the distance between the two subsets is made larger and larger. Because of the nearly exponential decay of the wavefunction $\Psi^{\alpha\beta}$ with the distance to the nuclei, it must tend to zero in the region between the two subsystems, and if we write the functions as an antisymmetrized product of functions at α and β

$$\Psi^{\alpha\beta}=\sum_{p}\sum_{p'}c_{pp'}\,\mathcal{A}(\Psi_p^{\alpha}\,\Psi_{p'}^{\beta}) \tag{18}$$

the overlap between Ψ_p^{α} and $\Psi_{p'}^{\beta}$ will be zero, so that

$$\rho^{\alpha\beta}(\mathbf{r})=\rho^{\alpha}(\mathbf{r})+\rho^{\beta}(\mathbf{r}) \tag{19}$$

$$\Gamma^{\alpha\beta}(\mathbf{r},\mathbf{r}')=\Gamma^{\alpha\alpha\,\alpha\alpha}(\mathbf{r},\mathbf{r}')+\Gamma^{\beta\beta\,\beta\beta}(\mathbf{r},\mathbf{r}')+\Gamma^{\alpha\alpha\,\beta\beta}(\mathbf{r},\mathbf{r}') \tag{20}$$

In the LCAO context, this means that the density will contain couples of basis functions centered either both at α or both at β, but there will appear no cross terms. Moreover, the pairs density will contain pairs of couples both centered at α, $\Gamma^{\alpha\alpha\,\alpha\alpha}(\mathbf{r},\mathbf{r}')$, or both at β, $\Gamma^{\beta\beta\,\beta\beta}(\mathbf{r},\mathbf{r}')$, or one at α and another at β, $\Gamma^{\alpha\alpha\,\beta\beta}(\mathbf{r},\mathbf{r}')$.

As a consequence of Eqs. (19) and (20), the terms associated to $\widehat{\mathcal{H}}^{\alpha\beta}_{\text{int}}$ in Eq. 9 will decay as powers of the inverses of the distances from the nuclei located at α and those at β and, because this is a smooth decay, there will be a wide region of the conformational space where overlap is negligible but interactions are not. This is the region where the interaction of the two systems is entirely determined by the Van der Waals forces.

Note that for very long distances, where not only overlap of Ψ_p^{α} with $\Psi_{p'}^{\beta}$ is almost zero, but also the interaction can be neglected, one has: $\Psi^{\alpha\beta}=\mathcal{A}(\Psi^{\alpha}\,\Psi^{\beta})$, and therefore

$$\rho^{\alpha\beta}(\mathbf{r})=\rho_{is}^{\alpha}(\mathbf{r})+\rho_{is}^{\beta}(\mathbf{r}) \tag{21}$$

$$\Gamma^{\alpha\beta}(\mathbf{r},\mathbf{r}')=\Gamma_{is}^{\alpha\alpha\,\alpha\alpha}(\mathbf{r},\mathbf{r}')+\Gamma_{is}^{\beta\beta\,\beta\beta}(\mathbf{r},\mathbf{r}')+\frac{1}{2}\left[\rho_{is}^{\alpha}(\mathbf{r})\,\rho_{is}^{\beta}(\mathbf{r}')+\rho_{is}^{\alpha}(\mathbf{r}')\,\rho_{is}^{\beta}(\mathbf{r})\right] \tag{22}$$

where is refers to isolated systems. Notice, by the way, that the asymptotic fulfillment of Eq. (22) is the condition for correct dissociation of a variational wavefunction.

The Van der Waals forces can be defined from the derivatives of the full energy $E_T^{\alpha\beta}$, with respect to the degrees of freedom that determine the relative position of the α and β systems, i.e., from the force and torque acting on them

$$\mathbf{F}^{\alpha}=\sum_{A\in\alpha}\mathbf{F}_A\quad\mathbf{F}^{\beta}=\sum_{B\in\beta}\mathbf{F}_B\quad\mathbf{F}^{\alpha}=-\mathbf{F}^{\beta} \tag{23}$$

$$\boldsymbol{\tau}^{\alpha}=\sum_{A\in\alpha}\mathbf{R}_A\times\mathbf{F}_A\quad\boldsymbol{\tau}^{\beta}=\sum_{B\in\beta}\mathbf{R}_B\times\mathbf{F}_B\quad\boldsymbol{\tau}^{\alpha}=-\boldsymbol{\tau}^{\beta} \tag{24}$$

where the last equalities come from Eqs. (7) and (8).

In order to gain insight on the relationship between the Van der Waals forces and the density, we will use Eqs. (11), (19) and (21), to rewrite the first equation of (23) which, taking into account that the net force on the isolated α system is zero, becomes

$$\mathbf{F}^{\alpha}=\sum_{A\in\alpha}\zeta_A\left[\int d\mathbf{r}\;\Delta\rho^{\alpha}(\mathbf{r})\,\frac{\mathbf{r}-\mathbf{R}_A}{|\mathbf{r}-\mathbf{R}_A|^3}+\int d\mathbf{r}\;\rho^{\beta}(\mathbf{r})\times\frac{\mathbf{r}-\mathbf{R}_A}{|\mathbf{r}-\mathbf{R}_A|^3}-\sum_{B\in\beta}\zeta_B\,\frac{\mathbf{R}_B-\mathbf{R}_A}{|\mathbf{R}_B-\mathbf{R}_A|^3}\right] \tag{25}$$

where

$$\Delta\rho^{\alpha}(\mathbf{r})=\rho^{\alpha}(\mathbf{r})-\rho_{is}^{\alpha}(\mathbf{r}) \tag{26}$$

In molecules, the two last terms of Eq. (25) cancel out almost completely, so that the small changes undergone by the density of each system due to the presence of the other become determinant.

A nice enlightening illustation is provided by the description of the Van der Waals forces of H_2 in terms of its density. As remarked above, at large distances, the density is almost zero in the region between the atoms and, therefore, it can be unambiguously expanded in real spherical harmonics—as defined in appendix—times radial factors at each nucleus

$$\rho^{\alpha\beta}(\mathbf{r}) = \sum_l \sum_m z_l^m(\mathbf{r}_\alpha) f_{lm}^\alpha(r_\alpha) + \sum_l \sum_m z_l^m(\mathbf{r}_\beta) f_{lm}^\beta(r_\beta) \tag{27}$$

with $\mathbf{r}_\alpha = \mathbf{r} - \mathbf{R}_\alpha$ and $\mathbf{r}_\beta = \mathbf{r} - \mathbf{R}_\beta$. This expansion stresses that the atomic densities, spherical for the isolated H atoms, will be deformed by the interaction. Notice that Eq. (27) is not an approximation but merely a representation of the density aimed at evincing its form: the terms with $l = 1$ describe the dipole-type deformation, those with $l = 2$, the quadrupole-type deformation, and so forth.

As a specific example, we have carried out a CISD calculation of the density of H_2 at an internuclear distance of 20 bohr with a [5,5,4,2,1] STO basis set using the SMILES [41–43] package for integrals and MOLPRO [44–48] for energy optimization. The density has been expanded with DAM [14–17], according to Eq. (27), yielding the terms with $l = 1, 2$ and 3 depicted in Fig. 1.

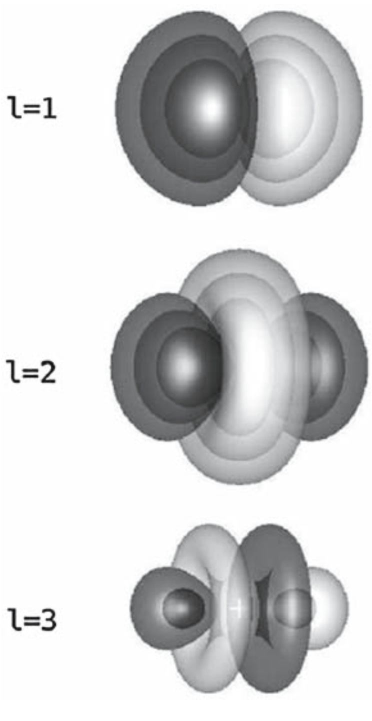

Fig. 1 Density deformations responsible for the Van der Waals forces in H_2 computed at CI level. Contour surfaces of $R^7\ z_l^0(\mathbf{r}_\alpha)\ f_{l0}(r_\alpha)$ for $l = 1, 2, 3$ at $R = 20$ bohr. *Contour values* 1, 1/3, 1/10. *Dark surface* charge accumulation; *light surface* charge depletion

Using Eq. (27), the force becomes

$$\begin{aligned}\mathbf{F}^\alpha &= \sum_l \sum_m \int \mathrm{d}\mathbf{r}\ z_l^m(\mathbf{r}_\alpha)\ f_{lm}^\alpha(r_\alpha)\ \frac{\mathbf{r}-\mathbf{R}_\alpha}{|\mathbf{r}-\mathbf{R}_\alpha|^3} \\ &\quad + \sum_l \sum_m \int \mathrm{d}\mathbf{r} z_l^m(\mathbf{r}_\beta) f_{lm}^\beta(r_\beta) \frac{\mathbf{r}-\mathbf{R}_\alpha}{|\mathbf{r}-\mathbf{R}_\alpha|^3} - \frac{\mathbf{R}_\beta-\mathbf{R}_\alpha}{|\mathbf{R}_\beta-\mathbf{R}_\alpha|^3}.\end{aligned} \tag{28}$$

Integrations of Eq. (28) are facilitated by adopting a lined up system with α *placed at the origin and* β *at a distance* R *on the negative* z *hemiaxis*. In such a system, it can be easily realized that $F_x^\alpha = 0$, $F_y^\alpha = 0$ and

$$\begin{aligned}F_z^\alpha &= \frac{4\pi}{3} \int_0^\infty \mathrm{d}r_\alpha\ r_\alpha\ f_{10}^\alpha(r_\alpha) \\ &\quad - \sum_{l=1}^\infty \frac{2}{R^{l+2}} \left[\frac{4\pi}{2l+1} \int_0^\infty \mathrm{d}r_\beta\ r_\beta^{2l+2}\ f_{l0}^\beta(r_\beta) \right]\end{aligned} \tag{29}$$

where $R = |\mathbf{R}_\beta - \mathbf{R}_\alpha|$, and the brackets are the multipolar moments Q_{l0}^β, of the cloud around nucleus β.

The first term in the r.h.s. of (28) is the force exerted by the charge distribution of atom H_α on its own nucleus. As it can be seen, this self-pulling (*internal*) force is entirely determined by the dipole-type term $z_1^0(\mathbf{r}_\alpha) f_{10}^\alpha(r_\alpha)$, of the density. The second and third terms are the force exerted by the H_β atom (cloud and nucleus) on nucleus α. At long distances, as considered here, the nucleus β is completely screened by the spherical part of its density and, therefore, the force exerted by this atom on nucleus α is due to the dipole, quadrupole and higher order terms of its density. The DAM package is also capable of solving the integrals of Eq. (29) and, for the density of the CISD calculation, it gives

$$F_z^\alpha(20) = -0.3299 \cdot 10^{-7} - 0.1062 \cdot 10^{-9} = -0.3309 \cdot 10^{-7} \tag{30}$$

all in atomic units (1au = 1 hartree/bohr). The first number is the value of the self-pulling force, and the second one, that of the external force. Clearly, the Van der Waals force is mainly determined by the self-pulling force, as advanced by Feynman almost seventy years ago [22]. The leading term in the series of Eq. (29), due to the dipole of β, $Q_{10}^\beta = 0.3404 \cdot 10^{-6}$ au at 20 bohr, gives a contribution of $-0.085 \cdot 10^{-9}$ au, which is only about a 0.2% of the total Van der Waals force.

Since one may have concerns about the adequacy of the CI method in this context, we have tested the CI results by comparing them with those of the perturbation theory. As noted in appendix, this theory allows one to write $f_{10}^\alpha(r_A)$ and $f_{10}^\beta(r_B)$ in the form

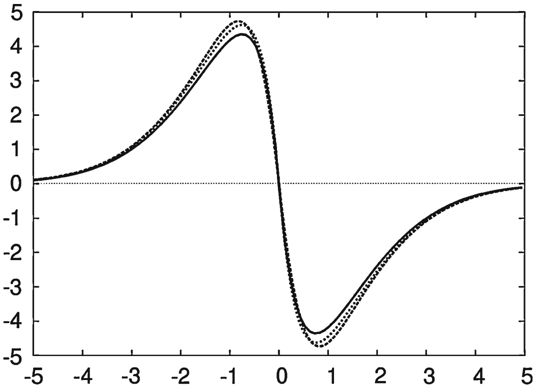

Fig. 2 Comparison of perturbative and CI dipole term in H_2. Values of $R^7\ z_1^0(\mathbf{r}_\alpha)\ f_{10}(r_\alpha)$ along the internuclear axis (z). *Dashed line* CI at $R = 25$ bohr; *dotted line* CI at $R = 20$ bohr; *solid line* perturbative

$$f_{10}^{\alpha}(r) = e^{-2r}\left[\frac{P_7(r)}{R^7} + \frac{P_9(r)}{R^9} + \cdots\right] \tag{31}$$

where $P_n(r) = \sum_{k=0}^{\infty} r^k\ c_k^{(n)}$ are power series independent of R, $c_k^{(n)}$ being numeric coefficients. The accurate calculation of the leading term $P_7(r)$, allows us to compare both approaches. In Fig. 2, the dipole-type deformations, $R^7\ z_1^0(\mathbf{r})\ f_{10}(r)$, obtained with CI calculations at $R = 20$ and $R = 25$ bohr are depicted together with the perturbative term $z_1^0(\mathbf{r})\ e^{-2r}\ P_7(r)$. It can be seen not only a reasonable agreement but also a correct convergence of the CI results towards the perturbative ones when increasing R. Moreover, using the perturbative result in Eq. (29) one has:

$$F_z^{\alpha}(R) \approx -\frac{1}{R^7}\ 38.99416023 - \frac{2}{R^{10}} \cdot 394.511. \tag{32}$$

Note that the first term contains the well known [49] 6 C_6 coefficient and the second is the contribution of the dipole Q_{10}^{β} in the series of Eq. (29). At $R = 20$ bohr, $Q_{10}^{\beta} = 0.3082\ 10^{-6}$ au, and

$$F_z^{\alpha}(20) \approx -0.3046 \cdot 10^{-7} - 0.0771 \cdot 10^{-10} = 0.3054 \cdot 10^{-7} \tag{33}$$

which must be compared with the values of Eq. (30) for the internal (self-pulling) and external components of the force. Comparison is satisfactory, bearing in mind the truncation of the perturbative solution to the term with $P_7(r)$—see Eq. (31)—and the absence, in the perturbative external force of multipoles higher than Q_{10} on atom β—see Eq. (29).

4 Pauli and bond forces in terms of density

At distances where overlap starts to be noticeable, new components coming from the two-center distributions appear in the density. They depend on the antisymmetry and spin of the wavefunction, and increase so rapidly with the overlap that, when distance decreases, they quickly dominate over Van der Waals forces.

In order to illustrate them, we will go back to the H_2 example. In this molecule, overlap becomes negligible at internuclear distances above 10 bohr. We have carried out CISD calculations using the aforementioned STO basis set in the range of distances between 7 and 10 bohr for the $^3\Sigma_u$ and $^1\Sigma_g$ states, and analyzed the density, finding that density deformations have now components coming from both the one- and two-center distributions. There is no problem to expand the first ones in spherical harmonic times radial factors. Moreover, the DAM package enables to expand the two-center distributions after partitioning them with the minimal deformation criterion. Figures 3 and 4 show separately the two contributions to the dipole-type deformations $z_1^0(\mathbf{r}) f_{10}(r)$, of the density in the triplet and singlet. Notice that this is the main deformation term because, as remarked above, it entirely determines the dominant self-pulling force and gives the main contribution to the interatomic force at these distances.

A glance at these figures is sufficient to see that the new terms play opposite roles in the triplet and singlet states. In the triplet the new component of the dipole term opposes to the previously existing one (associated to the attractive Van der Waals force) and generates a repulsive force that increases with the overlap, becoming quickly dominant when distance decreases.

On the contrary, in the singlet, the new component reinforces the Van der Waals force thus increasing the net attractive force when the atoms approach each other. Figure 5 shows the variation of net forces and energy with the internuclear distance for both states. We include Kolos' [50] results for comparison.

Repulsive forces associated to density deformations like that of the triplet will be called Pauli forces, whereas the attractive ones like in singlet are the so-called bond forces.

Since the terms associated to Pauli and bond forces are caused by antisymmetry and spin of the wavefunction, it is reasonable to expect qualitatively correct results, even from rough approximations to the wavefunction, provided that antisymmetry and spin are taken into account properly.

As an illustrating example, we will take the antisymmetrized spin-adapted products of the solutions of the isolated H atoms–see (22), which are the well known Heitler–London wavefunctions of H_2. Taking the function for the singlet, the density is

$$\rho_s^{\alpha\beta} = \frac{1}{1+\lambda^2}\ [a(\mathbf{r})\ a(\mathbf{r}) + b(\mathbf{r})\ b(\mathbf{r}) + 2\,\lambda\ a(\mathbf{r})\ b(\mathbf{r})] \tag{34}$$

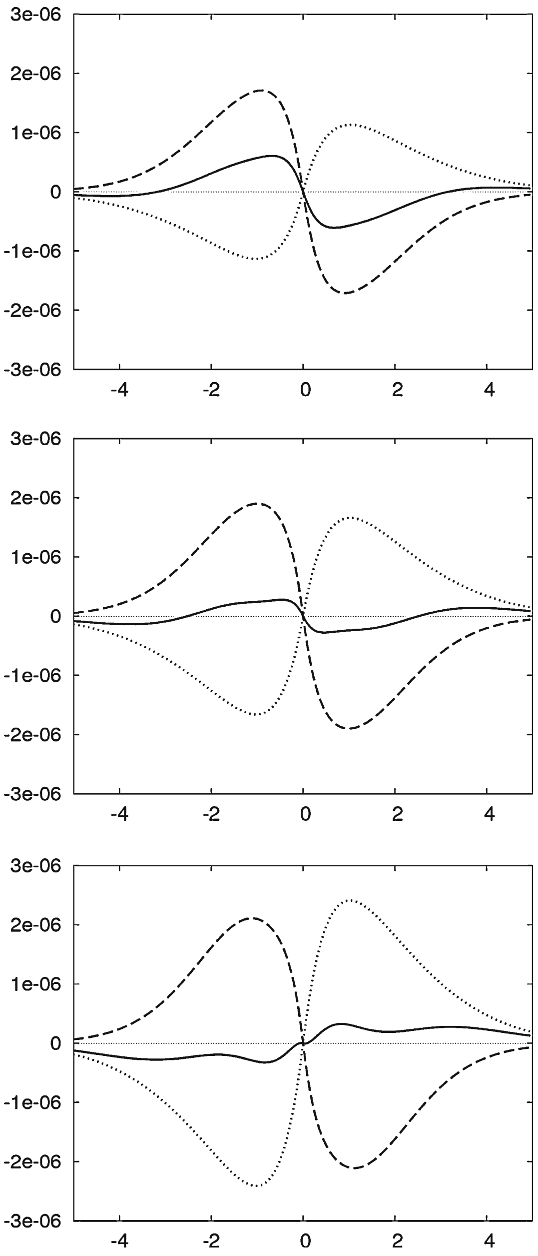

Fig. 3 Density deformations responsible for the Pauli forces in the $^3\Sigma_u$ of H_2. Contributions to the dipole term in electron/bohr^3. *Dotted lines* two-center, *dashed lines* one-center, *solid lines* total. *Upper* $R = 8.0$ bohr; *middle* $R = 7.8$ bohr; *lower* $R = 7.6$ bohr

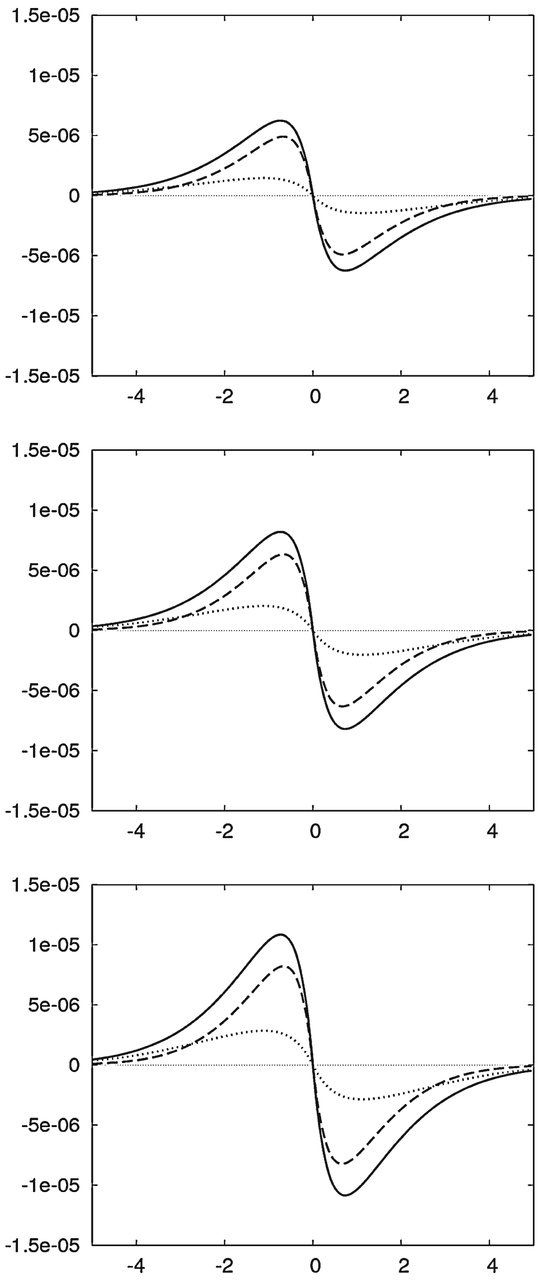

Fig. 4 Density deformations responsible for the bond forces in the $^1\Sigma_g$ of H_2. Contributions to the dipole term in electron/bohr^3. *Dotted lines* two-center, *dashed lines* one-center, *solid lines* total. *Upper* $R = 8.0$ bohr; *middle* $R = 7.8$ bohr; *lower* $R = 7.6$ bohr

and taking that of the triplet

$$\rho_t^{\alpha\beta} = \frac{1}{1-\lambda^2}\,[\,a(\mathbf{r})\,a(\mathbf{r}) + b(\mathbf{r})\,b(\mathbf{r}) - 2\,\lambda\,a(\mathbf{r})b(\mathbf{r})] \quad (35)$$

where $a(\mathbf{r}) = \left(\frac{\zeta^3}{\pi}\right)^{1/2} e^{-\zeta\, r_\alpha}$, $b(\mathbf{r}) = \left(\frac{\zeta^3}{\pi}\right)^{1/2} e^{-\zeta\, r_\beta}$, and $\lambda = \langle\, a(\mathbf{r})\,|\, b(\mathbf{r})\,\rangle$.

Using again a lined-up axis system, the force on α provided by this simple model is

$$F_z^\alpha(R) = \frac{1}{R} - \frac{1}{1\pm\lambda^2}\,\frac{\zeta^3}{\pi} \int \mathrm{d}\mathbf{r}\, \frac{z_1^0(\mathbf{r})}{r^3}\,\Big[e^{-2\zeta\, r} + e^{-2\zeta\, r_\beta} \pm 2\lambda\, e^{-\zeta\, r}\, e^{-\zeta\, r_\beta}\Big] \quad (36)$$

where the plus sign holds for singlet, and the minus for triplet. Expressions for all these integrals have been recently reported [51]. Using them, the force can be easily obtained as an explicit function of R and, by integrating the force with Eq. 12, the energy can be obtained as well. In order to give

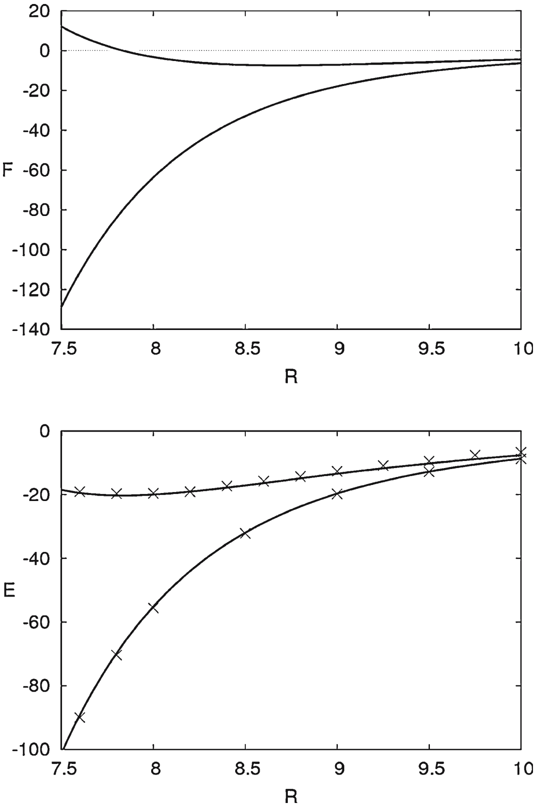

Fig. 5 Full CI net forces (*upper plate*) in μhartree/bohr, and energies (*lower plate*) in μhartree for the $^3\Sigma_u$ and $^1\Sigma_g$ of H_2. Kolos' energies ($\times$) included for comparison

an idea of what one can expect from this simple approach, we depict in Fig. 6 the force of Eq. (36) for the triplet (with $\zeta = 1$) together with the leading term, $-6C_6/R^7$, of the Van der Waals force and their sum. Moreover, we have included the CI reference force—see Fig. 5—for comparison. Clearly, although the simple Heitler–London density cannot describe the Van der Waals forces, it gives the correct trend for Pauli force.

The underlying idea of this approach is that the antisymmetrized spin-adapted products of the wavefunctions of the isolated systems give correct trends for the density deformations responsible for Pauli and bond forces. The extension of this idea would enable to carry out qualitative analysis and predictions of the forces acting on complex systems from simple models of the density. We will illustrate how this idea can be extended by means of a couple of examples.

Let α and β be two closed shell systems that, when isolated, are described by two closed shell determinants $\Psi^\alpha = |\phi_1^\alpha \overline{\phi}_1^\alpha \ldots \phi_{n_\alpha}^\alpha \overline{\phi}_{n_\alpha}^\alpha|$ and $\Psi^\beta = |\phi_1^\beta \overline{\phi}_1^\beta \ldots \phi_{n_\beta}^\beta \overline{\phi}_{n_\beta}^\beta|$. The antisymmetrized singlet product of these functions is

$$\Psi^{\alpha\beta} = |\phi_1^\alpha \overline{\phi}_1^\alpha \ldots \phi_{n_\alpha}^\alpha \overline{\phi}_{n_\alpha}^\alpha \, \phi_1^\beta \overline{\phi}_1^\beta \ldots \phi_{n_\beta}^\beta \overline{\phi}_{n_\beta}^\beta|. \qquad (37)$$

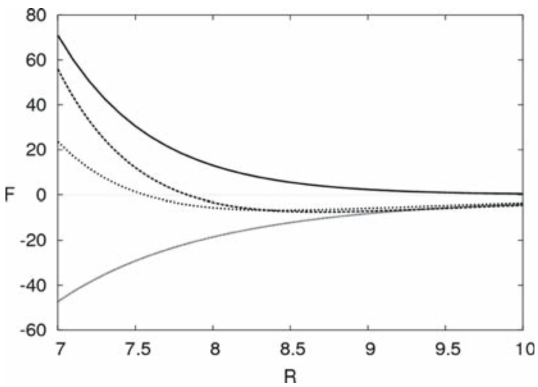

Fig. 6 Components of Pauli and Van der Waals forces (in μhartree/bohr) for the $^3\Sigma_u$ of H_2 according to the Heitler–London plus dispersion model. *Dark solid line* Pauli force; *light solid* dispersion; *dotted* net force. Full CI net force (*dashed*) included for comparison

Since this function is invariant under nonsingular transformations of the occupied orbitals, one can carry out rotations in the sets $\{\phi_i^\alpha\}_{i=1}^{n_\alpha}$ and $\{\phi_i^\beta\}_{i=1}^{n_\beta}$ to obtain new orbitals: $\{a_i\}_{i=1}^{n_\alpha}$, $\{b_i\}_{i=1}^{n_\beta}$ such that

$$\langle a_i \,|\, a_j \rangle = \delta_{ij} \quad \langle b_i \,|\, b_j \rangle = \delta_{ij} \quad \langle a_i \,|\, b_j \rangle = \lambda_i \, \delta_{ij}. \qquad (38)$$

In terms of these orbitals, the approximate wavefunction is

$$\Psi^{\alpha\beta} = |\, a_1 \, \overline{a}_1 \ldots a_{n_\alpha} \, \overline{a}_{n_\alpha} \, b_1 \, \overline{b}_1 \ldots b_{n_\beta} \, \overline{b}_{n_\beta} \,| \qquad (39)$$

and the density derived with the aid of Lowdin rules [52], assuming $n_\beta > n_\alpha$, is

$$\rho^{\alpha\beta}(\mathbf{r}) = \sum_{i=1}^{n_\alpha} \frac{2}{1-\lambda_1^2} \left[a_i(\mathbf{r})\, a_i(\mathbf{r}) + b_i(\mathbf{r})\, b_i(\mathbf{r}) \right.$$
$$\left. -2\,\lambda_i \; a_i(\mathbf{r})\, b_i(\mathbf{r}) \right] + \sum_{i=n_\alpha+1}^{n_\alpha+n_\beta} 2\, b_i(\mathbf{r})\, b_i(\mathbf{r}) \qquad (40)$$

Clearly, the overlapping orbitals ($\lambda_i \neq 0$) behave very much like those of the triplet of H_2—see Eq. (35)— and, therefore, the associated density deformations must generate Pauli forces.

As a specific illustration, we have used the Hartree–Fock wavefunction [53] of the isolated He in Eq. (39) to approximate the Pauli forces of the He_2 system as a function of R. Results are depicted in Fig. 7 together with the leading term of the Van der Waals force [54,55], $-\frac{6c_6}{R^7}$, and their sum. Moreover, the energy was obtained by integrating the force. This simple model predicts a well with a deep of 23 μhartree at $R_e = 5.83$ bohr. The currently accepted values [54,55] are 34.7 μhartree and 5.61 bohr, so that the approximate results are qualitatively correct and quantitatively not too bad, given the crudeness of the model.

As a second example, we will consider two radicals that approach each other to form a closed shell molecule with a single bond. Assuming that the radicals are described by

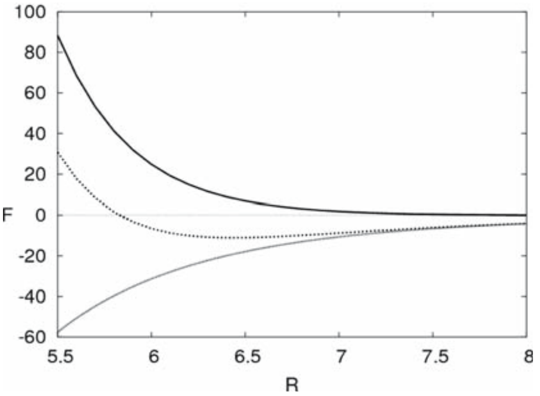

Fig. 7 Competence between Pauli and Van der Waals forces (in μhartree/bohr) for the $^1\Sigma_g$ of He_2 according to the Heitler–London plus dispersion model. *Dark solid line* Pauli force; *light solid* dispersive force; *dotted* net force

single open-shell restricted Hartree–Fock (OSRHF) determinants: $\Psi^\alpha = |\phi_1^\alpha \phi_2^\alpha \overline{\phi}_2^\alpha \ldots \phi_{n_\alpha}^\alpha \overline{\phi}_{n_\alpha}^\alpha|$ and $\Psi^\beta = |\phi_1^\beta \phi_2^\beta \overline{\phi}_2^\beta \ldots \phi_{n_\beta}^\beta \overline{\phi}_{n_\beta}^\beta|$, and carrying out the biorthogonalization of both sets of occupied orbitals—Eq. (38)— the adduct wavefunction for the singlet can be written as

$$\Psi^{\alpha\beta} = |a_1 a_2 \overline{a}_2 \ldots a_{n_\alpha} \overline{a}_{n_\alpha} \overline{b}_1 b_2 \overline{b}_2 \ldots b_{n_\beta} \overline{b}_{n_\beta}| \\ - |\overline{a}_1 a_2 \overline{a}_2 \ldots a_{n_\alpha} \overline{a}_{n_\alpha} b_1 b_2 \overline{b}_2 \ldots b_{n_\beta} \overline{b}_{n_\beta}|. \quad (41)$$

Now, applying Lowdin rules and taking into account Eq. (38) one obtains

$$\rho^{\alpha\beta} = \frac{1}{1+\lambda_1^2}[a_1(\mathbf{r})a_1(\mathbf{r}) + b_1(\mathbf{r})b_1(\mathbf{r}) + 2\lambda_1 a_1(\mathbf{r})b_1(\mathbf{r})] \\ + \sum_{i=2}^{n_\alpha} \frac{2}{1-\lambda_1^2}\,[a_i(\mathbf{r})\,a_i(\mathbf{r}) + b_i(\mathbf{r})\,b_i(\mathbf{r}) \\ -2\,\lambda_i\; a_i(\mathbf{r})\,b_i(\mathbf{r})\,] + \sum_{i=n_\alpha+1}^{n_\alpha+n_\beta} 2\,b_i(\mathbf{r})\,b_i(\mathbf{r}). \quad (42)$$

It is evident from this expression that overlapping orbitals of the closed shells give, as in the previous case, density deformations that generate Pauli forces, but the orbitals in the open shell behave just like those of the singlet of H_2—Eq. (34)—and, therefore, yield bond forces. Clearly, the behavior of these systems will be ruled by the competition between their Pauli and bond forces, and their structure relaxations can be predicted on the basis that it must tend to follow these forces, a process which necessarily will lower the energy.

To illustrate this, we will consider two methyl radicals faced to one another at a distance $R_{CC} = 3.5$ bohr (larger than the equilibrium distance). OSRHF calculations with the VB1 STO basis set [56] (again with SMILES and MOLPRO) give for isolated radical CH_3 a planar structure with R_{CH} =2.042 bohr. Taking the OSRHF function of the isolated methyl groups in Eqs. (41) and (42), a rough density can be obtained whose forces, schematized in the upper plate of Fig. 8, tend to bend the C–C–H angle. The CAS (2,2) calculation with this basis set gives at zero Pauli force (the minimum of energy for this C–C distance) a C–C–H angle of 107° —see lower plate of Fig. 8—so that, once again, the simple model gives the correct trend.

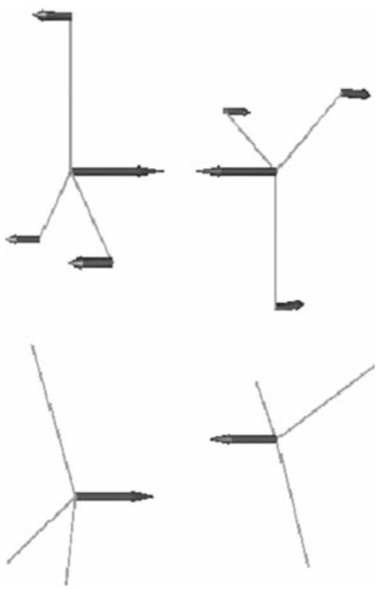

Fig. 8 Competence between Pauli and bond forces in two faced methyl groups at $R_{CC} = 3.5$ bohr: planar (*upper*) and released (*lower*) conformations. Forces in arbitrary units

5 Nuclear unscreening

According to Eq. 11, every nucleus is repelled by the other nuclei and attracted by the electron cloud. As the electron density is strongly localized around the nuclei, for nuclei placed far away, the repulsive effect of their charges will be almost completelly cancelled out by the cloud around them. However, the electron screening will decrease as the nuclei approach each other and the corresponding repulsive forces will increase without any bound. These repulsive contributions will be called *nuclear unscreening forces*, and play an important role in determining the molecular conformations, because they impede the nuclear collapse under the effect of bond forces.

In order to better understand these forces, it is convenient to consider a partition of the density into fragments associated to nuclei

$$\rho(\mathbf{r}) = \sum_A \rho^A(\mathbf{r}) \quad (43)$$

whose detailed shapes are irrelevant provided that Eq. (43) is fulfilled and that every fragment bears almost all the charge distribution around its associated nucleus. Once the partition has been made, the density of each fragment can be separated

$$\rho^A(\mathbf{r}_A) = \rho_{00}^A(r_A) + \Delta_A(\mathbf{r}) \tag{44}$$

in a spherical part which, after integration over the whole space, gives the total charge of $\rho^A(\mathbf{r}_A)$

$$\rho_{00}^A(r_A) = \frac{1}{4\pi} \int_0^{2\pi} \mathrm{d}\phi_A \int_0^{\pi} \sin\theta_A \, \mathrm{d}\theta_A \; \rho^A(\mathbf{r}) \tag{45}$$

and a deformation part $\Delta_A(\mathbf{r})$, containing terms other than the spherical one, which integrate to zero. By combining Eqs. (43), (45) with (11), one obtains

$$\mathbf{F}_A = \zeta_A \sum_B \int \mathrm{d}\mathbf{r} \; \Delta^B(\mathbf{r}) \; \frac{\mathbf{r} - \mathbf{R}_A}{|\mathbf{r} - \mathbf{R}_A|^3} \\ -\zeta_A \sum_{B \neq A} \zeta_B^{\mathrm{eff}} \; \frac{\mathbf{R}_B - \mathbf{R}_A}{|\mathbf{R}_B - \mathbf{R}_A|^3} \tag{46}$$

where

$$\zeta_B^{\mathrm{eff}} = \zeta_B - 4\pi \int_0^{|\mathbf{R}_A - \mathbf{R}_B|} \mathrm{d}\mathbf{r}_B \; r_B^2 \; \rho_{00}^B(r_B). \tag{47}$$

The first term in the r.h.s. of Eq. (46) determines how the force on A is affected by the deformation of the clouds around the nuclei. As discussed above, it determines the Van der Waals forces at long distances, and Pauli and bond forces at intermediate ones.

The second term gives the components of the force due to the spherical parts of the clouds. These are the *nuclear unscreening forces*, the simplest ones of the four types. They are directed along the internuclear axis, necessarily repulsive for $|\mathbf{R}_B - \mathbf{R}_A|$ small, and quickly increase boundless as $|\mathbf{R}_B - \mathbf{R}_A|$ tends to zero.

Since the spherical terms contain *all the electronic charge*, at medium distances, the unscreening forces take the form of *charge transfer forces* which can be easily understood from the simple Gauss theorem. Note in particular that, if $\rho_{00}^B(r_B)$ is everywhere positive, as it must be, a fragment B with zero or positive net charge has $\zeta_B^{\mathrm{eff}} > 0$ and, therefore, its contribution to the second term of Eq. (46) will be repulsive. However, if B has negative net charge, the nature of this contribution depends on the distance $|\mathbf{R}_A - \mathbf{R}_B|$. At sufficiently long distance ζ_B^{eff} will be the negative charge of B—see Eq. (47)—$\zeta_B^{\mathrm{eff}} < 0$, and the contribution in Eq. (46) is attractive but, since the integral of Eq. (46) decays with $|\mathbf{R}_A - \mathbf{R}_B|$, at small distance $\zeta_B^{\mathrm{eff}} > 0$ and the contribution to (46) is repulsive.

It must be stressed that, due to the absence of cloud to cloud interactions in the Hellmann–Feynman context, the conventional ideas about the electrostatic forces involving ions must be carefully reviewed. As an illustrative example, we will consider a pair formed by positive and negative spherical ions. According to the previous discussion, in the Hellmann–Feynman framework the positive ion repells the nucleus of the negative partner at all distances, whereas this latter will attract the former at long separation but repell it at short distance.

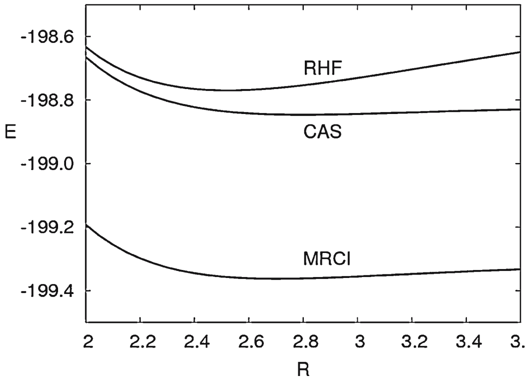

Fig. 9 Energy of F_2 as a function of the internuclear distance at RHF, CAS and MRCI levels

In the conventional electrostatic view, each ion is regarded as a cloud-nucleus unit and all interaction forces are taken into account, including the repulsion between clouds. However, this repulsion makes sense only in a two-electron interaction which is completely absent in the Hellmann–Feynman framework, a fact that is not always considered [57].

As an illustrative example we choose here the F_2 molecule. Energy curves obtained from RHF, valence CAS and MRCI (including all single and double excitations over valence CAS) are plotted in Fig. 9. They were computed with the FVB1 STO basis set, using again SMILES for STO integrals and MOLPRO for energy optimization.

The difficulties in computations of this molecule are widely known. The RHF curve lies entirely over the RHF energy of the separated atoms and has a minimum at a too short distance: $R_e(RHF) = 2.52$ bohr. The CAS curve is qualitatively correct, with $R_e(CAS) = 2.80$ bohr, slightly longer than the experimental value [58]: $R_e(\exp) = 2.71$ bohr, and the well depth, about 16 kcal mol^{-1}, is much smaller than the experimental value [58], of 38.3 kcal mol^{-1}. The MRCI gives the correct equilibrium distance $R_e(MRCI) = 2.71$ bohr but the well depth—about 30 kcal mol^{-1}—is still low.

These difficulties can be predicted from the analysis of the forces. The F_2 molecule is isoelectronic to ethane and, therefore, like in this, there is a competence between valence Pauli and bond forces. However, since Pauli forces cannot be minimized by means of a conformational relaxation, this minimization is accomplished through a relaxation of the electronic structure whose description requires high level calculations.

The atomic density deformations of F_2 –$\Delta_A(\mathbf{r})$ of Eq. (44) given by DAM– plotted in Fig. 10 exhibit a dominant quadrupole type shape. Since this quadrupole deformation yields

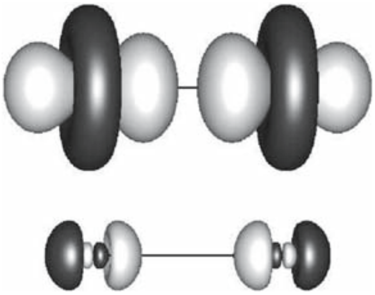

Fig. 10 Density deformations of F_2 (*upper*) and its dipole components (*lower*) from the MRCI density at the equilibrium distance. Countour surface of ±0.04 electron/bohr^3

repulsive external forces and zero internal force, in absence of terms other than quadrupole, the molecule could not be stable. A more detailed decomposition of $\Delta\rho(\mathbf{r})$ in terms with $l = 1, 2, \ldots$ shows—see lower plate of Fig. 10—small dipole terms with two lobes embedded in $\Delta\rho(\mathbf{r})$. The innermost is sharply concentrated close to the nucleus, yieldig attractive forces, whereas the outermost is diffuse and repulsive. The internal net force results from the balance of the opposite effects of these terms, and is attractive because the first term dominates over the second.

Note, by the way, that this rearrangement of the charge in the binding region yields attractive forces without the charge transfer from antibinding to binding regions required by Berlin's condition [6], a fact first recognized by Spackman [59].

Figure 11 shows the forces acting on a nucleus of F_2 as computed with the DAM package from the RHF, CAS and MRCI densities. The components of the force arising from density deformations (upper plate) and those coming from the spherical part of the cloud (nuclear unscreening force, lower plate) are depicted separately. The repulsive curve of Fig. 11 (upper plate) is mainly the external force caused by the quadrupole-type deformation, and is clearly incorrect in case of RHF. Attraction is due to self-pulling, i.e., to the dipole term of the density deformations, thus coming from the subtle balance of the two opposite effects discussed above. Since these forces are sensitive to errors in the small density deformations, high level calculations are required to obtain accurate results. This sensitiveness contrasts with the strong stability against changes in the computational level of the nuclear unscreening forces shown in Fig. 11 (lower plate). As stressed above, the nuclear unscreening forces are quantitatively correct even for the basically wrong RHF density.

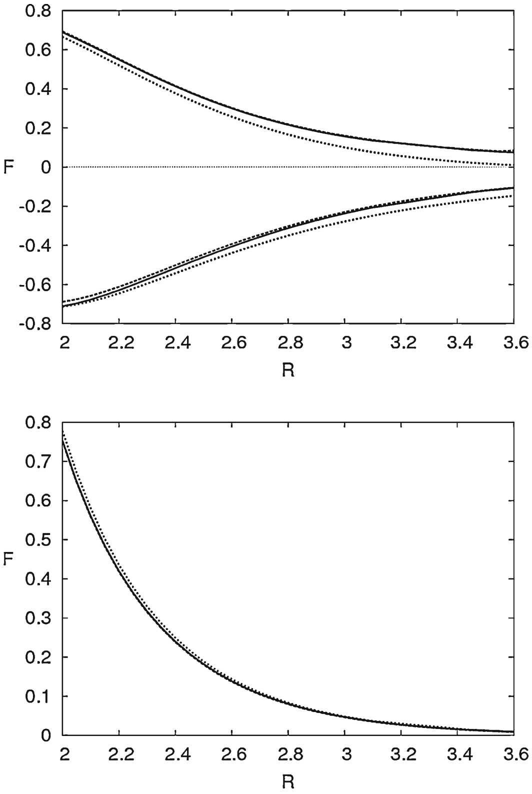

Fig. 11 Forces on nuclei (hartree/bohr) of F_2 as functions of the internuclear distance for RHF (*dotted lines*), CAS (*dashed*) and MRCI (*solid*) densities. *Upper plate* external repulsive (positive) and self-pulling (negative) forces caused by the density deformations. *Lower plate* nuclear unscreening forces

6 Conclusions

The attractive Van der Waals and bond forces and the repulsive Pauli forces are mainly caused by the small deformations produced in the atomic densities by the molecular environment, and can be related to the self-pulling of the nuclei by the dipole-type terms imbedded in these deformations.

The nuclear unscreening forces are due to the spherical clouds around the nuclei. At medium distances they take the form of charge transfer forces between positive and negative pairs, that cannot produce stable systems and, at short distances, they are repulsive.

The interaction of two stable closed shell molecules or atoms in the region of low (but not negligible) overlap of their wavefunctions is determined by the competence between Van der Waals and Pauli forces. Models for density obtained from the antisymmetrized spin-adapted products of simple wavefunctions of the isolated monomers are often sufficient to give correct approximations to Pauli forces. Therefore, if approximations to Van der Waals forces are available, one can make reasonable predictions on the geometry and stability of Van der Waals complexes.

At moderate distances (near equilibrium) Pauli, bond and nuclear unscreening forces compete. Since the latter depend on the spherical parts of the clouds, their effects can be easily understood from Gauss theorem and can be easily described by rough wavefuntions, so that their values are almost insensitive to the method employed for computing the density. On the contrary, the small density deformations that cause the Pauli and bond forces can be strongly dependent on the environment and high level calculation are often needed to obtain correct descriptions.

Chemical forces depend on the density and every partition of density in chemically meaningful contributions is accompanied by the corresponding decomposition of the forces and conversely. Obviously, this decomposition is not unique, and a particular choice is a matter of mere convenience.

The partition chosen herein is aimed at supporting on density the forces usually employed in chemistry. Van der Waals, bond and Pauli forces, which belong to the common chemical language—though the latter are controversial [60–63]—are herein associated to specific deformations of the density. Nuclear unscreening forces are not usually considered but are necessary in order to complete the total force.

We note finally that, in the Hellmann–Feynman approach, all this four types of forces are rooted in the density, thus having a similar conceptual support. In a different approach, in which for instance the separation of the total force into components is considered useless, one may say that *Pauli repulsions exist only in the eye of the beholder* [62] but, with similar arguments, the existence of bond forces, Van der Waals and so forth can be likewise denied. This is clearly a perspective that sets the results of Quantum Mechanics far away from chemical intuition.

Acknowledgment This article is dedicated to the memory of Prof. Serafín Fraga, whose contributions to the development of Quantum Chemistry have been widely recognized, and whose enthusiastic support, encouraging suggestions, warm personality and priceless friendship have left us an indelible memory.

Appendix: Dipole-type deformation on H_2 from perturbation theory

The standard perturbative equations can be written in the form

$$(H^{(0)}-E^{(0)})\psi^{(n)} = (E^{(1)}-V)\psi^{(n-1)} + \sum_{i=2}^{n} E^{(i)}\psi^{(n-i)} \tag{48}$$

where $E^{(i)}$ and $\psi^{(i)}$ are the successive corrections to energy and wavefunction, and $H^{(0)}$ and V are the zeroth order hamiltonian and perturbation operator, respectively. The perturbation operator is given in Eq. 17, and for H_2 at large distance reads

$$V = \sum_{l=1}^{\infty}\sum_{l'=1}^{\infty}\sum_{m=-l_<}^{l_<} \frac{(2-\delta_{m,0})(l+l')!(-1)^{l'+|m|}}{(l+|m|)!(l'+|m|)!} \times \frac{z_l^m(\mathbf{r})\, z_{l'}^m(\mathbf{r}')}{R^{l+l'+1}} \tag{49}$$

with the real spherical harmonics defined by

$$\begin{aligned} z_l^m(\mathbf{r}) &= r^l\, z_l^m(\mathbf{r}/r) \\ &= r^l\, (-1)^m\, P_l^m(\cos\theta)\, \cos(m\phi) \quad m \geq 0 \\ z_l^m(\mathbf{r}) &= r^l\, z_l^m(\mathbf{r}/r) \\ &= r^l\, (-1)^{|m|}\, P_l^{|m|}(\cos\theta)\, \sin(|m|\phi)\ m < 0. \end{aligned} \tag{50}$$

Grouping together the perturbative terms with the same power of R, the wavefunction can be written as

$$\psi = \sum_{k=0}^{\infty} \frac{\phi^{(k)}}{R^k} \tag{51}$$

where $\phi^{(k)}$ can be expanded in products of spherical harmonics times radial factors which, in turn, are expressed as symmetrized products of exponentials times series of Laguerre polynomials

$$\phi^{(k)} = \sum_{ll'} \phi_{ll'}^{(k)} \tag{52}$$

where

$$\phi_{ll'}^{(k)} = \widehat{\mathcal{S}} \sum_{m=-l}^{l} \sum_{m'=-l'}^{l'} z_l^m(\mathbf{r})\, z_{l'}^{m'}(\mathbf{r}')\, e^{-r-r'} \times \sum_{p}^{p_{\max}} \sum_{q}^{p_{\max}} c_{pq}^{(k)lml'm'} L_p^{2l_1+1}(2r) L_q^{2l_2+1}(2r') \tag{53}$$

and $\widehat{\mathcal{S}}$ is the symmetrizer.

In this way, the perturbative Eq. (48) take the form

$$(H^{(0)}-E^{(0)})\phi^{(k)} = \sum_{lm}\sum_{l'm'} z_l^m(\mathbf{r})\, z_{l'}^{m'}(\mathbf{r}')\, F_{lml'm'}^{(k)}(r,r') \times e^{-r-r'} \tag{54}$$

and, after projection in the same basis of spherical harmonics times Laguerre functions, the $c_{pq}^{(k)lml'm'}$ are obtained solving a linear system of equations.

To obtain the non-vanishing contribution of order R^{-7} to the dipole term of the density, $\rho_{10}(\mathbf{r})$, one needs the first order, $\phi_{11}^{(3)}$, $\phi_{21}^{(4)}$, and second order, $\phi_{10}^{(7)}$, corrections. Thus, one has

$$\rho_{10}(\mathbf{r}) = \frac{2}{R^7}\frac{3}{4\pi r}\left\{ z_1^0(\mathbf{r}_\alpha) \int_0^{2\pi} \mathrm{d}\phi_\alpha \int_0^{\pi} \mathrm{d}\theta_\alpha\, \sin\theta_\alpha\, z_1^0(\mathbf{r}_\alpha/r_\alpha) \right.$$

$$\times \int_{0}^{\infty} \mathrm{d}\mathbf{r}' \left[\phi_{11}^{(3)}(\mathbf{r},\mathbf{r}')\phi_{21}^{(4)}(\mathbf{r},\mathbf{r}') + \phi_{00}^{(0)}(\mathbf{r},\mathbf{r}')\phi_{10}^{(7)}(\mathbf{r},\mathbf{r}') \right]$$

$$+ z_1^0(\mathbf{r}_\beta) \int_{0}^{2\pi} \mathrm{d}\phi_\beta \int_{0}^{\pi} \mathrm{d}\theta_\beta \sin\theta_\beta \; z_1^0(\mathbf{r}_\beta / r_\beta)$$

$$\times \int_{0}^{\infty} \mathrm{d}\mathbf{r}' \left[\phi_{11}^{(3)}(\mathbf{r},\mathbf{r}')\, \phi_{21}^{(4)}(\mathbf{r},\mathbf{r}') + \phi_{00}^{(0)}(\mathbf{r},\mathbf{r}')\, \phi_{10}^{(7)}(\mathbf{r},\mathbf{r}') \right] \Bigg\}$$

$$= \frac{1}{R^7} \left[z_1^0(\mathbf{r}_\alpha)\, e^{-2r_\alpha} P_7(r_\alpha) + z_1^0(\mathbf{r}_\beta)\, e^{-2r_\beta}\; P_7(r_\beta) \right] \tag{55}$$

where $P_7(r)$ is a power series of r as defined in the main text.

In practice, $p_{\max}$ of Eq. (53) was increased in order to attain convergence in the $P_7(r)$ series up to eight decimal figures.

References

1. Clementi E (2005) Attempting to simulate large molecular systems In: Dykstra C et al (ed) Theory and applications of computational chemistry: The first years. Elsevier, Amsterdam, pp 89–114
2. Coulson CA (1960) Rev Mod Phys 32:170–177
3. Hurley AC (1955) Proc Phys Soc A 68:149–155
4. Hurley AC (1956) 69:49–56
5. Hurley AC (1956) 69:301–309
6. Berlin T (1951) J Chem Phys 19:208–213
7. Politzer P (1965) J Phys Chem 69:2132–2134
8. Politzer P (1966) J Phys Chem 70:1174–1178
9. Bader RFW, Jones GA (1961) Can J Chem 39:1253–1265
10. Bader RFW, Preston HJT (1966) Can J Chem 44:1131–1145
11. Bader RFW, Chandra AK (1968) Can J Chem 46:953–966
12. Stone AJ (1966) The theory of intermolecular forces. Clarendon, Oxford
13. Deb BM (1981) The force concept in chemistry. Van Nostrand, New York
14. Fernández Rico J, López R, Ramírez G (1999) J Chem Phys 110:4213–4220
15. Fernández Rico J, López R, Ema I, Ramírez G (2002) J Chem Phys 117:533–540
16. Fernández Rico J, López R, Ema I, Ramírez G, Ludeña EV (2004) J Comput Chem 25:1355–1363
17. Fernández Rico J, López R, Ema I, Ramírez G (2004) J Comput Chem 25:1347–1354
18. Fernández Rico J, López R, Ramírez G, Ema I (2003) J Chem Phys 119:12251–12256
19. Fernández Rico J, López R, Ema I, Ramírez G (2005) J Mol Struct Theochem 727:115–121
20. Fernández Rico J, López R, Ema I, Ramírez G (2004) Int J Quantum Chem 100:221–230
21. Fernández Rico J, López R, Ema I, Ramírez G (2007) J Comput Chem 28:748–758
22. Feynman RP (1939) Phys Rev 56:340
23. Hellmann H (1937) Einführung in die Quantemchemie. Deuticke, Leipzig
24. Fernández Rico J, López R, Ema I, Ramírez G (2002) J Chem Phys 116:1788–1799
25. Fernández Rico J, López R, Ema I, Ramírez G (2006) J Chem Theory Comput 106:1986–1997
26. Slater JC (1972) J Chem Phys 57:2389–2396
27. Epstein S, Hurley AC, Wyatt RE, Parr RG (1967) J Chem Phys 47:1275–1286
28. Parr RG (1964) J Chem Phys 40:3726
29. Kim H, Parr RG (1964) J Chem Phys 41:2892–2897
30. Moscardó F (2006) Chem Phys Lett 428:187–190
31. Hirschfelder JO, Curtiss CF, Bird RB (1964) Molecular theory of gases and liquids. Wiley, New York, p 933
32. Pulay P (1969) Mol Phys 17:197
33. Hall GG (1961) Philos Mag 6:249
34. Frost AA (1967) J Chem Phys 47:3707–3713
35. Cohen M, Dalgarno A (1961) Proc Phys Soc London 77:748
36. Stanton RE (1962) J Chem Phys 36:1298–1300
37. Tuan DF (1969) J Chem Phys 51:607–611
38. Coulson CA (1971) Mol Phys 20:687
39. Nakatsuji H, Parr RG (1975) J Chem Phys 63:1112–1117
40. Bakken V, Helgacker T, Klopper W, Ruud K (1999) Mol Phys 96:653–671
41. Fernández Rico J, López R, Aguado A, Ema I, Ramírez G (1998) J Comput Chem 19:1284–1293
42. Fernández Rico J, López R, Aguado A, Ema I, Ramírez G (2001) Int J Quantum Chem 81:148–153
43. Fernández Rico J, López R, Ema I, Ramírez G (2004) J Comput Chem 25:1987–1994
44. Amos RD, Bernhardsson A, Berning A, Celani P, Cooper DL, Deegan MJO, Dobbyn AJ, Eckert F, Hampel C, Hetzer G, Knowles PJ, Korona T, Lindh R, Lloyd AW, McNicholas SJ, Manby FR, Meyer W, Mura ME, Nicklaß A, Palmieri P, Pitzer R, Rauhut G, Schütz M, Schumann U, Stoll H, Stone AJ, Tarroni R, Thorsteinsson T, Werner H-J In: Werner H-J, Knowles PJ (eds) MOLPRO a package of ab initio programs. version 2002.5
45. Werner HJ, Knowles PJ (1985) J Chem Phys 82:5053–5063
46. Knowles PJ, Werner HJ (1985) Chem Phys Lett 115:259–267
47. Werner HJ, Knowles PJ (1988) J Chem Phys 89:5803–5814
48. Knowles PJ, Werner HJ (1988) Chem Phys Lett 145:514–522
49. Mitroy J, Bromley MWJ (2005) Phys Rev A 71:032709–032709-5
50. Kolos W, Wolniewicz L (1965) J Chem Phys 43:2429–2441
51. Fernández Rico J, López R, Ema I, Ramírez G (2006) Int J Quantum Chem 106:1986–1997
52. McWeeny R (1989) Methods of molecular quantum mechanics. Academic, New York
53. Clementi E, Roetti C (1974) At Data Nucl Data Tables 14:177
54. Aziz RA, Janzen AR, Moldover MR (1995) Phys Rev Lett 74:1586–1589
55. Hättig C, Larsen H, Olsen J, Jorgensen P, Koch H, Fernández B, Rizzo A (1999) J Chem Phys 111:10099–10107
56. Ema I, Garcíadela Vega JM, Ramírez G, López R, Fernández Rico J, Meißner H, Paldus J (2003) J Comput Chem 24:859–868
57. Ma Y, Politzer P (2004) J Chem Phys 120:8955–8959
58. Huber KP, Herzberg G (1979) Molecular spectra and molecular structure IV:constants of diatomic molecules. Van Nostrand, New York
59. Spackman MA, Maslen EN (1985) Acta cryst Sect A 41:347
60. Matta CF, Hernández Trujillo J, Tang T, Bader RFW (2003) Chem Eur J 9:1940–1951
61. Poater J, Solà M, Bickelhaupt FM (2006) Chem Eur J 12:2889–2895
62. Bader RFW (2006) Chem Eur J 12:2896–2901
63. Poater J, Solà M, Bickelhaupt FM (2006) Chem Eur J 12:2902–2905